MARTIN MARIETTA ENERGY SYSTEMS LIBRARIES

3 4456 0266194 7

ORNL/TM-10223

ornl

OAK RIDGE
NATIONAL
LABORATORY

MARTIN MARIETTA

ICRF Heating in a Straight, Helically Symmetric Stellarator

E. F. Jaeger
H. Weitzner
D. B. Batchelor

OAK RIDGE NATIONAL LABORATORY
CENTRAL RESEARCH LIBRARY
CIRCULATION SECTION
4500N ROOM 175
LIBRARY LOAN COPY
DO NOT TRANSFER TO ANOTHER PERSON
If you wish someone else to see this report, send in name with report and the library will arrange a loan.

OPERATED BY
MARTIN MARIETTA ENERGY SYSTEMS, INC.
FOR THE UNITED STATES
DEPARTMENT OF ENERGY

Printed in the United States of America. Available from
National Technical Information Service
U.S. Department of Commerce
5285 Port Royal Road, Springfield, Virginia 22161
NTIS price codes—Printed Copy: A03; Microfiche A01

This report was prepared as an account of work sponsored by an agency of the United States Government. Neither the United States Government nor any agency thereof, nor any of their employees, makes any warranty, express or implied, or assumes any legal liability or responsibility for the accuracy, completeness, or usefulness of any information, apparatus, product, or process disclosed, or represents that its use would not infringe privately owned rights. Reference herein to any specific commercial product, process, or service by trade name, trademark, manufacturer, or otherwise, does not necessarily constitute or imply its endorsement, recommendation, or favoring by the United States Government or any agency thereof. The views and opinions of authors expressed herein do not necessarily state or reflect those of the United States Government or any agency thereof.

ORNL/TM-10223
Dist. Category UC-20 g

Fusion Energy Division

ICRF HEATING IN A STRAIGHT, HELICALLY SYMMETRIC STELLARATOR

E. F. Jaeger
H. Weitzner[a]
D. B. Batchelor

[a]Courant Institute of Mathematical Sciences, New York University, New York, N.Y. 10012

DATE PUBLISHED — July 1987

Prepared by the
OAK RIDGE NATIONAL LABORATORY
Oak Ridge, Tennessee 37831
operated by
MARTIN MARIETTA ENERGY SYSTEMS, INC.
for the
U.S. DEPARTMENT OF ENERGY
under contract DE-AC05-84OR21400

MARTIN MARIETTA ENERGY SYSTEMS LIBRARIES
3 4456 0266194 7

CONTENTS

ACKNOWLEDGMENT v

ABSTRACT vii

1 INTRODUCTION 1

2 THE STRAIGHT, HELICALLY SYMMETRIC STELLARATOR . . . 2
2.1 DIELECTRIC TENSOR REPRESENTATION 3
2.2 WAVE EQUATION—STELLARATOR 4

3 MODEL STELLARATOR MAGNETIC FIELD 7

4 LOCAL ENERGY DEPOSITION AND ANTENNA IMPEDANCE . . 8

5 NUMERICAL RESULTS 10

REFERENCES 19

ACKNOWLEDGMENT

The authors wish to acknowledge very helpful discussions with our colleagues P. L. Colestock, K. Appert, and K. Imre.

ABSTRACT

Experimental observations of direct ion cyclotron resonant frequency (ICRF) heating at fundamental ion cyclotron resonance on the L-2 stellarator have stimulated interest in the theoretical basis for such heating. In this paper, global solutions for the ICRF wave fields in a helically symmetric, straight stellarator are calculated in the cold plasma limit. The component of the wave electric field parallel to $\vec{B}$ is assumed zero. Helical symmetry allows Fourier decomposition in the longitudinal (z) direction. The two remaining partial differential equations in r and $\phi \equiv \theta - hz$ (h is the helical pitch) are solved by finite differencing. Energy absorption and antenna impedance are calculated from an ad hoc collision model. Results for parameters typical of the L-2 and Advanced Toroidal Facility (ATF) stellarators show that direct resonant absorption of the fundamental ion cyclotron resonance occurs mainly near the plasma edge. The magnitude of the absorption is about half that for minority heating at the two-ion hybrid resonance.

1 INTRODUCTION

Recent measurements in the U.S.S.R. on the L-2 stellarator have demonstrated efficient heating of a pure hydrogen plasma ($n_e \sim 1\text{–}2\times10^{13}\,\mathrm{cm}^{-3}$) with ion cyclotron resonant heating (ICRH) power in the range of the first harmonic of the ion cyclotron frequency [1]. Since conventional theory for tokamak plasmas shows that heating at the fundamental ion cyclotron resonance is ineffective [2], there has been some interest [3,4] in understanding the theoretical basis for the observed fundamental heating on L-2. Kovrizhnykh and Moroz [3] study mode structure for the fast magnetosonic wave in a cylindrical metal waveguide filled with plasma. The assumed magnetic field is uniform in the axial direction, and the applied frequency equals the ion cyclotron frequency everywhere. They find that for $10^{13} < n_{\mathrm{av}} < 3.8\times10^{13}\,\mathrm{cm}^{-3}$ (as in L-2), only the $m = 1$ mode exists, E_+ is a surface wave, and significant heating is possible only near the plasma edge. For $n > 3.8\times10^{13}\,\mathrm{cm}^{-3}, m = (0, 2)$ modes can also be excited with secondary maxima for E_+ inside the plasma. This implies heating inside the plasma as well. The same authors show that, in stellarators [4], the helical structure of $\vec{B}$ can lead to absorption that is enhanced compared with that in tokamaks with similar plasma parameters.

In this report, we address the question of fundamental heating in stellarators by extending the full-wave calculations for tokamaks and mirrors [2] to the case of a straight, helically symmetric stellarator. Global solutions of the ion cyclotron resonant frequency (ICRF) wave fields are found numerically in the cold plasma limit for parameters typical of the L-2 and Advanced Toroidal Facility (ATF) stellarators. The component of the wave electric field parallel to $\vec{B}$ is assumed zero, and helical symmetry is used to Fourier decompose the solution in the longitudinal (z) direction. The remaining set of two coupled, two-dimensional partial differential equations in r and $\phi \equiv \theta - hz$ (h is the helical pitch) is solved by finite differencing. Energy absorption and antenna impedance are calculated from an ad hoc collisional model. Similar calculations for parameters typical of Heliotron-E and ATF have been carried out in Japan by Fukayama et al. [5] using finite element analysis and including parallel electric fields. Fukayama et al. [5], however, consider only the case of minority heating at the two-ion hybrid resonance. We also consider direct heating of the majority ions at the fundamental ion cyclotron frequency and compare the results to similar cases of minority heating at the two-ion hybrid resonance.

Section 2 reviews the assumptions of helical symmetry and describes the decomposition of the cold plasma dielectric tensor into components along unit tensors in flux coordinates. The wave equation for the straight, helically symmetric stellarator is developed in Sect. 2.2, and the reduced set of two partial differential equations, which are solved numerically, is displayed in detail. These are shown to reduce exactly to the equations for a tokamak when $h = 0$ and $B_r = 0$. In Sect. 3, the model magnetic field for an $\ell = 2$ stellarator is developed, and expressions for energy deposition and antenna impedance are derived in Sect. 4. Section 5 describes numerical results for L-2 and ATF parameters and compares minority heating at the two-ion hybrid to majority heating at the fundamental ion cyclotron resonance.

2 THE STRAIGHT, HELICALLY SYMMETRIC STELLARATOR

In the helically symmetric system, it is useful to transform from cylindrical coordinates (r, θ, z) to helical coordinates (r, ϕ, z') where $\phi = \theta - hz$, $z' = z$, and $h = 2\pi/L_p$, where L_p is the helical field periodic length in z. Note that $\phi = \text{const}$ is the equation of a helix. Helical symmetry requires that the unperturbed magnetic field $\vec{B}_0$ be a function only of r and ϕ but not z'; that is, the field at one point in space depends only on which helix that point is on and not on its position in z. Writing $\nabla \cdot \vec{B}_0 = 0$ in helical coordinates (r, ϕ, z') and requiring $\vec{B}_0$ to be independent of z' (helical symmetry) gives

$$\begin{aligned} B_r^0 &= \frac{1}{r}\frac{\partial \psi}{\partial \phi}, \\ B_\theta^0 - hrB_z^0 &= -\frac{\partial \psi}{\partial r}, \end{aligned} \tag{1}$$

where $\psi(r, \phi)$ is the scalar flux function for $\vec{B}_0(r, \phi)$,

$$\psi(r, \phi) = \int_0^\phi rB_r^0 d\phi, \tag{2}$$

and $\phi_B = \int_0^{2\pi/h} dz' \psi(r, \phi) = (2\pi/h)\psi(r, \phi)$ is the magnetic flux through a helical surface. Likewise, $\nabla \cdot \vec{J} = 0$ in (r, ϕ, z') coordinates with $\vec{J}$ independent of z' gives

$$\begin{aligned} \mu_0 J_r &= \frac{1}{r}\frac{\partial \chi}{\partial \phi}, \\ \mu_0\left(J_\theta - hrJ_z\right) &= -\frac{\partial \chi}{\partial r}, \end{aligned} \tag{3}$$

where $\chi(r, \phi)$ is the scalar flux function for the plasma current $J(r, \phi)$. Now from $\mu_0 \vec{J} = \nabla \times \vec{B}_0$ written in (r, ϕ, z')

$$\begin{aligned} \mu_0 J_r &= \frac{1}{r}\frac{\partial}{\partial \phi}\left(B_z^0 + hrB_\theta^0\right), \\ \mu_0\left(J_\theta - hrJ_z\right) &= -\frac{\partial}{\partial r}\left(B_z^0 + hrB_\theta^0\right). \end{aligned} \tag{4}$$

Comparing Eqs. (3) and (4) gives

$$\chi(r, \phi) = B_z^0 + hrB_\theta^0. \tag{5}$$

Combining Eqs. (1) and (3) with Eq. (5), we can write the helically symmetric magnetic field $\vec{B}_0(r, \phi)$ and current density $\vec{J}(r, \phi)$ in terms of the flux functions ψ and χ as

$$\vec{B}_0 = \frac{\psi_{,\phi}}{r}\hat{r} - \frac{\psi_{,r}(\hat{\theta} - hr\hat{z})}{1 + h^2r^2} + \frac{\chi(\hat{z} + hr\hat{\theta})}{1 + h^2r^2}, \tag{6}$$

$$\mu_0 \vec{J} = \frac{\chi_{,\phi}}{r}\hat{r} - \frac{\chi_{,r}(\hat{\theta} - hr\hat{z})}{1 + h^2r^2} + \left[\frac{2h\chi}{(1 + h^2r^2)^2} - \Delta^*\psi\right](\hat{z} + hr\hat{\theta}), \tag{7}$$

where the notation $f_{,x}$ means the partial derivative of f with respect to x, $\partial f/\partial x$, and

$$\Delta^* \psi = \frac{1}{r}\frac{\partial}{\partial r}\left(\frac{r}{1+h^2r^2}\frac{\partial \psi}{\partial r}\right) + \frac{1}{r}\frac{\partial^2 \psi}{\partial \phi^2} \quad .$$

From Eq. (6) we get

$$(1+h^2r^2)\left|\vec{B}_0\right|^2 = \chi^2 + |\nabla\psi|^2 \, . \tag{8}$$

With $p = p(\psi)$, the $\nabla\psi$ component of the equation of force balance is

$$|\nabla\psi|^2 \frac{\partial p}{\partial \psi} = \nabla\psi \cdot \vec{J} \times \vec{B}_0 \, .$$

Then substituting Eqs. (6), (7), and (8) for $\vec{B}_0$, $\vec{J}$, and $|\nabla\psi|^2$ and using $\chi = \chi(\psi)$, we find

$$\Delta^* \psi = -\mu_0 p'(\psi) + \frac{2h\chi}{(1+h^2r^2)^2} - \frac{\chi'(\psi)\chi}{1+h^2r^2} \, ,$$

which is the Grad-Shafranov equation for helical symmetry.

2.1 DIELECTRIC TENSOR REPRESENTATION

We now choose the right-hand orthogonal coordinate system with unit vectors:

$$\begin{aligned}
\hat{\delta}_1 &= \widehat{\nabla\psi} = \frac{1}{|\nabla\psi|}\left[\psi_{,r}\hat{r} + \frac{\psi_{,\phi}}{r}\left(\hat{\theta} - hr\hat{z}\right)\right] , \\
\hat{\delta}_2 &= \hat{b} \times \widehat{\nabla\psi} = \frac{1}{|\nabla\psi|\,|B_0|}\left[|B_0|^2\left(\hat{z} + hr\hat{\theta}\right) - \chi\vec{B}_0\right] , \\
\hat{\delta}_3 &= \hat{b} = \frac{1}{|B_0|}\left[\frac{\psi_{,\phi}}{r}\hat{r} - \frac{\psi_{,r}\left(\hat{\theta} - hr\hat{z}\right)}{1+h^2r^2} + \frac{\chi\left(\hat{z} + hr\hat{\theta}\right)}{1+h^2r^2}\right] ,
\end{aligned} \tag{9}$$

where the circumflex ˆ denotes a vector of unit magnitude. Now $\overleftrightarrow{K} \cdot \vec{E}$ can be written

$$\begin{aligned}
\overleftrightarrow{K} \cdot \vec{E} = \hat{\delta}_1(K_{xx}\hat{\delta}_1 \cdot \vec{E} + K_{xy}\hat{\delta}_2 \cdot \vec{E} + K_{xz}\hat{\delta}_3 \cdot \vec{E}) \\
+ \hat{\delta}_2(K_{yx}\hat{\delta}_1 \cdot \vec{E} + K_{yy}\hat{\delta}_2 \cdot \vec{E} + K_{yz}\hat{\delta}_3 \cdot \vec{E}) \\
+ \hat{\delta}_3(K_{zx}\hat{\delta}_1 \cdot \vec{E} + K_{zy}\hat{\delta}_2 \cdot \vec{E} + K_{zz}\hat{\delta}_3 \cdot \vec{E}) \, .
\end{aligned} \tag{10}$$

Now, assuming $\hat{\delta}_3 \cdot \vec{E} = \hat{b} \cdot \vec{E} = 0$, we have

$$E_z = -\frac{B_r^0}{B_z^0}E_r - E_\theta \frac{B_\theta^0}{B_z^0} \, . \tag{11}$$

The components of $\vec{E}$ perpendicular to $\vec{B}$ are defined as

$$\begin{aligned}
E_\psi &\equiv \hat{\delta}_1 \cdot \vec{E} = \frac{1}{|\nabla\psi|}\left[E_r\left(\psi_{,r} + hr\frac{B_r^{0^2}}{B_z^0}\right) + E_\theta \chi \frac{B_r^0}{B_z^0}\right] , \\
E_\chi &= \hat{\delta}_2 \cdot \vec{E} = \frac{|B_0|}{|\nabla\chi|}\left(-E_r\frac{B_r^0}{B_z^0} + E_\theta\frac{\psi_{,r}}{B_z^0}\right) \, .
\end{aligned} \tag{12}$$

Equation (10) now gives

$$\overleftrightarrow{K}\cdot\vec{E} = \hat{\delta}_1(K_{xx}E_\psi + K_{xy}E_\chi) + \hat{\delta}_2(K_{yx}E_\psi + K_{yy}E_\chi) + \hat{\delta}_3(K_{zx}E_\psi + K_{zy}E_\chi)\,, \tag{13}$$

where in the cold plasma limit

$$K_{xx} = K_{yy} = K_\perp = 1 - \sum_j \frac{w_{pj}^2}{w^2 - \Omega_j^2}\,,$$

$$K_{xy} = -K_{yx} = -iK_x = -i\sum_j \frac{\Omega_j}{\omega}\frac{\omega_{pj}^2}{\omega^2 - \Omega_j^2}\,,$$

$$K_{zx} = K_{zy} = 0\,.$$

Also from Eqs. (11), (1), and (5) we find

$$E_z + hrE_\theta = -E_r\frac{B_r^0}{B_z^0} + E_\theta\frac{\psi_{,r}}{B_z^0} = E_\chi\frac{|\nabla\psi|}{|B_0|}\,,$$

$$E_\theta - hrE_z = hrE_r\frac{B_r^0}{B_z^0} + E_\theta\frac{\chi}{B_z^0} = E_\psi\frac{|\nabla\psi|}{B_r^0} - E_r\frac{\psi_{,r}}{B_r^0}\,.$$

2.2 WAVE EQUATION—STELLARATOR

We now write the $\hat{\delta}_1 = \widehat{\nabla\psi}$ and $\hat{\delta}_2 = \hat{b}\times\widehat{\nabla\psi}$ components of the wave equation,

$$-\nabla\times\nabla\times\vec{E} + (\omega^2/c^2)\overleftrightarrow{K}\cdot\vec{E} = -i\omega\mu_0\vec{J}_{\text{ext}}\,.$$

This gives

$$-i\omega\widehat{\nabla\psi}\cdot\nabla\times\vec{B} + \frac{\omega^2}{c^2}\widehat{\nabla\psi}\cdot\overleftrightarrow{K}\cdot\vec{E} = -i\omega\mu_0\widehat{\nabla\psi}\cdot\vec{J}_{\text{ext}}\,, \tag{14}$$

$$-i\omega\hat{b}\times\widehat{\nabla\psi}\cdot\nabla\times\vec{B} + \frac{\omega^2}{c^2}\hat{b}\times\widehat{\nabla\psi}\cdot\overleftrightarrow{K}\cdot\vec{E} = -i\omega\mu_0\hat{b}\times\widehat{\nabla\psi}\cdot\vec{J}_{\text{ext}}\,, \tag{15}$$

where we have replaced $\nabla\times\vec{E}$ with $i\omega\vec{B}$ for convenience. The terms $\widehat{\nabla\psi}\cdot\overleftrightarrow{K}\cdot\vec{E}$ and $\hat{b}\times\widehat{\nabla\psi}\cdot\overleftrightarrow{K}\cdot\vec{E}$ are given by Eq. (13). To write the $\widehat{\nabla\psi}\cdot\nabla\times\vec{B}$ and $\hat{b}\times\widehat{\nabla\psi}\cdot\nabla\times\vec{B}$ terms, we Fourier analyze $\vec{E}$ and $\vec{J}_{\text{ext}}$ as

$$\vec{E}(r,\phi,z') = \sum_{k_z} E_{k_z}(r,\phi)e^{ik_z z'}\,,$$
$$\vec{J}_{\text{ext}}(r,\phi,z') = \sum_{k_z} J_{k_z}(r,\phi)e^{ik_z z'} \tag{16}$$

and write $\nabla\times\vec{B} = (1/i\omega)\nabla\times\nabla\times\vec{E}$ in helical coordinates:

$$\begin{aligned}\nabla\times\vec{B} = &\left[\frac{1}{r}\frac{\partial}{\partial\phi}(B_z + hrB_\theta) - ik_zB_\theta\right]\hat{r}\\ &+ [ik_zB_r - \frac{\partial}{\partial r}(B_z + hrB_\theta)](\hat{\theta} - hr\hat{z})\\ &+ \left[\frac{1}{r}\frac{\partial(rB_\theta - hr^2B_z)}{\partial r} + 2hB_z - \frac{(1+h^2r^2)}{r}\frac{\partial B_r}{\partial\phi} + ihk_zrB_r\right](\hat{z} + hr\hat{\theta})\,.\end{aligned} \tag{17}$$

Then from Eq. (9),

$$\widehat{\nabla\psi}\cdot\nabla\times\vec{B} = \frac{\psi_{,r}}{|\nabla\psi|}\left[\frac{1}{r}\frac{\partial(B_z+hrB_\theta)}{\partial\phi} - ik_zB_\theta\right] + \frac{\psi_{,\phi}}{r|\nabla\psi|}\left[ik_zB_r - \frac{\partial(B_z+hrB_\theta)}{\partial r}\right], \tag{18}$$

$$\begin{aligned}\hat{b}\times\widehat{\nabla\psi}\cdot\nabla\times\vec{B} = \frac{1}{|B_0||\nabla\psi|}\Bigg\{&\frac{|\nabla\psi|^2}{1+h^2r^2}\left[\frac{1}{r}\frac{\partial r(B_\theta-hrB_z)}{\partial r} + 2hB_z\right.\\ &\left.-\frac{1+h^2r^2}{r}\frac{\partial B_r}{\partial\phi} + ihk_zrB_r\right]\\ &+\frac{\chi\psi_{,r}}{1+h^2r^2}\left[ik_zB_r - \frac{\partial(B_z+hrB_\theta)}{\partial r}\right]\\ &-\frac{\chi\psi_{,\phi}}{r}\left[\frac{1}{r}\frac{\partial(B_z+hrB_\theta)}{\partial\phi} - ik_zB_\theta\right]\Bigg\},\end{aligned} \tag{19}$$

and Eqs. (14) and (15) become (multiplying by $|\nabla\psi|$)

$$\begin{aligned}&-i\omega\left[\frac{\psi_{,r}}{r}\frac{\partial(B_z+hrB_\theta)}{\partial\phi} - \frac{\psi_{,\phi}}{r}\frac{\partial(B_z+hrB_\theta)}{\partial r} + ik_z\left(\frac{\psi_{,\phi}}{r}B_r - \psi_{,r}B_\theta\right)\right]\\ &+\frac{\omega^2}{c^2}K_\perp\left[E_r\left(\psi_{,r}+hr\frac{B_r^{0\,2}}{B_z^0}\right) + E_\theta\chi\frac{B_r^0}{B_z^0}\right] - \frac{\omega^2}{c^2}iK_x|B_0|\left(-E_r\frac{B_r^0}{B_z^0} + E_\theta\frac{\psi_{,r}}{B_z^0}\right)\\ &= -i\omega u_0\left[\psi_{,r}J_r + \frac{\psi_{,\phi}}{r}(J_\theta - hrJ_z)\right],\end{aligned} \tag{20}$$

$$\begin{aligned}&-\frac{i\omega}{|B_0|}\frac{|\nabla\psi|^2}{1+h^2r^2}\left[\frac{1}{r}\frac{\partial(rB_\theta-hr^2B_z)}{\partial r} + 2hB_z - \frac{1+h^2r^2}{r}\frac{\partial B_r}{\partial\phi} + ihk_zrB_r\right]\\ &-\frac{i\omega\chi}{|B_0|}\left[\frac{-\psi_{,r}}{1+h^2r^2}\frac{\partial(B_z+hrB_\theta)}{\partial r} - \frac{\psi_{,\phi}}{r^2}\frac{\partial(B_z+hrB_\theta)}{\partial\phi}\right.\\ &\left.+ik_z\left(\frac{\psi_{,r}B_r}{1+h^2r^2} + \frac{\psi_{,\phi}B_\theta}{r}\right)\right]\\ &+\frac{\omega^2}{c^2}K_\perp|B_0|\left(-E_r\frac{B_r^0}{B_z^0} + E_\theta\frac{\psi_{,r}}{B_z^0}\right) + \frac{\omega^2}{c^2}iK_x\left\{E_r\left[\psi_{,r} + hr\frac{(B_r^0)^2}{B_z^0}\right] + E_\theta\chi\frac{B_r^0}{B_z^0}\right\}\\ &= -i\omega\mu_0\frac{1}{|B_0|}\left[|B_0|^2(J_z+hrJ_\theta) - \chi\vec{B}_0\cdot\vec{J}_{\text{ext}}\right].\end{aligned} \tag{21}$$

In Eqs. (20) and (21), $\nabla\times\vec{E}$ is written for brevity as $i\omega\vec{B}$. We now replace $i\omega\vec{B}$ with $\nabla\times\vec{E}$

in helical coordinates. Eliminating E_z with Eqs. (11) and (12) gives

$$
\begin{aligned}
i\omega\vec{B} = \nabla\times\vec{E} = &\left[\frac{1}{r}\frac{\partial}{\partial\phi}\left(-E_r\frac{B_r^0}{B_z^0}+\frac{E_\theta\psi_{,r}}{B_z^0}\right)-ik_zE_\theta\right]\hat{r}\\
&+\left[-h\frac{\partial E_r}{\partial\phi}+ik_zE_r+\frac{\partial}{\partial r}\left(E_r\frac{B_r^0}{B_z^0}+E_\theta\frac{B_\theta^0}{B_z^0}\right)\right]\hat{\theta}\\
&+\frac{1}{r}\left[\frac{\partial rE_\theta}{\partial r}-\frac{\partial E_r}{\partial\phi}\right]\hat{z}\,.
\end{aligned}
\tag{22}
$$

From Eq. (22) we find also

$$
\begin{aligned}
i\omega\left(B_\theta-hrB_z\right) &= ik_zE_r+\frac{\partial}{\partial r}\left(E_r\frac{B_r^0}{B_z^0}+E_\theta\frac{B_\theta^0}{B_z^0}\right)-h\frac{\partial rE_\theta}{\partial r}\,,\\
i\omega\left(B_z+hrB_\theta\right) &= \frac{1}{r}\frac{\partial rE_\theta}{\partial r}+hr\frac{\partial}{\partial r}\left(E_\theta\frac{B_\theta^0}{B_z^0}+E_r\frac{B_r^0}{B_z^0}\right)-\frac{1+h^2r^2}{r}\frac{\partial E_r}{\partial\phi}+ihk_zrE_r\,.
\end{aligned}
\tag{23}
$$

Thus, with the definitions $u = rE_r$ and $v = rE_\theta$, Eqs. (20) and (21) become

$$
\begin{aligned}
&-\frac{1}{r}\frac{\partial^2 v}{\partial\phi\partial r}-\frac{hr}{R_{\mathrm{T}}}\frac{\partial^2(\hat{\imath}v+\alpha u)}{\partial\phi\partial r}+\frac{1+h^2r^2}{r^2}\frac{\partial^2 u}{\partial\phi^2}-2ihk_z\frac{\partial u}{\partial\phi}\\
&+\frac{\alpha}{\kappa}\left[r\frac{\partial}{\partial r}\left(\frac{1}{r}\frac{\partial v}{\partial r}\right)+\frac{hr}{R_{\mathrm{T}}}\frac{\partial}{\partial r}r\frac{\partial(\hat{\imath}v+\alpha u)}{\partial r}-r\frac{\partial}{\partial r}\left(\frac{1+h^2r^2}{r^2}\right)\frac{\partial u}{\partial\phi}+ihrk_z\frac{\partial u}{\partial r}\right]\\
&+\frac{ik_z}{R_{\mathrm{T}}}\left[\frac{\alpha}{\kappa}\frac{\partial(\alpha u-\kappa v)}{\partial\phi}+r\frac{\partial(\alpha u+\hat{\imath}v)}{\partial r}\right]\\
&+\left\{\frac{\omega^2}{c^2}\left[K_{zx}\left(1+hr\frac{\alpha}{\kappa}\frac{b_r}{b_z}\right)-\frac{K_{zy}}{b_z}\frac{\alpha}{\kappa}\right]-k_z^2\right\}u\\
&+\left[\frac{\omega^2}{c^2}\left(K_{zx}\frac{\alpha}{\kappa}\frac{\hat{\chi}}{b_z}+\frac{K_{zy}}{b_z}\right)-\frac{\alpha}{\kappa}k_z^2\right]v=-i\omega\mu_0r\left[J_r+\frac{\alpha}{\kappa}(J_\theta-hrJ_z)\right],
\end{aligned}
\tag{24}
$$

$$
\begin{aligned}
&\left(1+hr\frac{|\nabla\hat{\psi}|^2}{\hat{\psi}_{,r}\hat{\chi}}\right)\left[r\frac{\partial}{\partial r}\left(\frac{1}{r}\frac{\partial v}{\partial r}\right)-\frac{ik_z}{R_{\mathrm{T}}}\frac{\partial(v\kappa-\alpha u)}{\partial\phi}\right]\\
&\quad+\left(hr-\frac{|\nabla\hat{\psi}|^2}{\hat{\psi}_{,r}\hat{\chi}}\right)\left[\frac{1}{R_{\mathrm{T}}}\frac{\partial}{\partial r}r\frac{\partial(\hat{\imath}v+\alpha u)}{\partial r}+ik_z\frac{\partial u}{\partial r}\right]\\
&\quad+\left(\frac{|\nabla\hat{\psi}|^2}{\hat{\psi}_{,r}\hat{\chi}}\frac{1+h^2r^2}{r}\right)\left[\frac{1}{R_{\mathrm{T}}}\frac{\partial^2(\kappa v-\alpha u)}{\partial\phi^2}-ik_z\frac{\partial v}{\partial\phi}\right]\\
&\quad+\left[\frac{|\nabla\hat{\psi}|^2}{\hat{\psi}_{,r}\hat{\chi}}+\frac{\alpha}{\kappa}(1+h^2r^2)ik_zr\right]\frac{2h}{r}\frac{\partial u}{\partial\phi}\\
&\quad-r\frac{\partial}{\partial r}\left(\frac{1+h^2r^2}{r^2}\frac{\partial u}{\partial\phi}\right)+\frac{\alpha}{\kappa}(1+h^2r^2)\left[\frac{1}{r}\frac{\partial^2 v}{\partial\phi\partial r}+\frac{hr}{R_{\mathrm{T}}}\frac{\partial^2(\hat{\imath}v+\alpha u)}{\partial\phi\partial r}\right.\\
&\quad\left.-\frac{1+h^2r^2}{r^2}\frac{\partial^2 u}{\partial\phi^2}-\frac{ik_zr}{R_{\mathrm{T}}}\frac{\partial(\alpha u+\hat{\imath}v)}{\partial r}\right]
\end{aligned}
$$

$$+\frac{1+h^2r^2}{\hat{\psi}_{,r}\hat{\chi}}\left\{\frac{\omega^2}{c^2}\left[-K_{yy}\frac{b_r}{b_z}+K_{yx}\left(\hat{\psi}_{,r}+hr\frac{b_r^2}{b_z}\right)\right]+\hat{\chi}b_rk_z^2\right\}u$$

$$+\left[\frac{1+h^2r^2}{\hat{\psi}_{,r}b_z}\frac{\omega^2}{c^2}\left(K_{yy}\frac{\hat{\psi}_{,r}}{\hat{\chi}}+K_{yx}b_r\right)-k_z^2\left(1+hr\frac{|\nabla\hat{\psi}|^2}{\hat{\psi}_{,r}\hat{\chi}}\right)\right]v$$

$$=-iw\mu_0r\frac{1+h^2r^2}{\hat{\psi}_{,r}\hat{\chi}}\left[J_z(1-\hat{\chi}b_z)+J_\theta(hr-\hat{\chi}b_\theta)-J_r(\hat{\chi}b_r)\right], \tag{25}$$

where in the cold plasma limit $K_{xx}=K_{yy}=K_\perp$, $K_{xy}=-K_{yx}=-iK_x$, $K_{zx}=K_{zy}=0$; $\hat{\chi}=b_z+hrb_\theta$, $\hat{\psi}_{,r}=-b_\theta+hrb_z$, $|\nabla\hat{\psi}|^2=\hat{\psi}_{,r}^2+b_r^2(1+h^2r^2)$; and

$$\begin{aligned}\alpha&=\frac{R_T}{r}\frac{b_r}{b_z},\\ \hat{\iota}&=\frac{R_T}{r}\frac{b_\theta}{b_z},\\ \kappa&=\frac{R_T}{r}\frac{\hat{\psi}_{,r}}{b_z}=hR_T-\hat{\iota}\,.\end{aligned} \tag{26}$$

R_T is the major radius. Note that $\hat{\iota}$ is a local quantity and thus does not correspond to the usual definition of rotational transform in stellarators. We note that if $\alpha=0$ and $h=0$, then $\phi=\theta$, $\kappa=-\hat{\iota}$, $\hat{\psi}_{,r}=-b_\theta$, $\hat{\chi}=b_z$, and $|\nabla\hat{\psi}|^2=b_\theta^2$ so that Eqs. (24) and (25) reduce to the equations for a tokamak [6].

Boundary conditions for the solution of Eqs. (24) and (25) are that the tangential component of $\vec{E}$ should vanish at $r=R$. This gives $rE_\theta=v=0$ and $E_z=0$ at $r=R$, so that from Eq. (11) we also have $rE_r=u=0$ at $r=R$. Also, we use periodicity in ϕ to give $u(\phi=0)=u(\phi=2\pi)$ and $v(\phi=0)=v(\phi=2\pi)$.

3 MODEL STELLARATOR MAGNETIC FIELD

To solve Eqs. (24) and (25) we take the helical flux functions ψ and χ in Eqs. (2) and (5) to be [7,8]

$$\begin{aligned}\psi(r,\phi)&=B_0\frac{hr^2}{2}-r\sum_\ell\varepsilon_\ell I_\ell'(\ell hr)\cos\ell\phi\,,\\ \chi(r,\phi)&=B_0=\text{const}\,,\end{aligned} \tag{27}$$

where I_ℓ is the modified Bessel function of order ℓ. Then from Eq. (6)

$$\begin{aligned}B_r^0&=\frac{1}{r}\frac{\partial\psi}{\partial\phi}=\sum_\ell\ell\varepsilon_\ell I_\ell'(\ell hr)\sin\ell\phi\,,\\ B_\theta^0&=\frac{-\partial\psi/\partial r+hr\chi}{1+h^2r^2}=\frac{1}{hr}\sum_\ell\ell\varepsilon_\ell I_\ell(\ell hr)\cos\ell\phi\,,\\ B_z^0&=\frac{hr(\partial\psi/\partial r)+\chi}{1+h^2r^2}=B_0-\sum_\ell\ell\varepsilon_\ell I_\ell(\ell hr)\cos\ell\phi\,,\end{aligned} \tag{28}$$

where we have used Bessel's equation $z^2I_\ell''(z)+zI_\ell'(z)+(z^2+\ell^2)I_\ell=0$ to find that

$$\frac{\partial}{\partial r}rI_\ell'(\ell hr)=\frac{\ell}{hr}(1+h^2r^2)I_\ell(\ell hr)\,.$$

For the case of the $\ell = 2$ stellarator, the helical terms are dominated by the $\ell = 2$ term in Eqs. (27) and (28), which matches the external winding number. In this case the coefficients occurring in Eqs. (24) and (25) are

$$\alpha = \frac{R_T}{r}\frac{b_r}{b_z} = \begin{cases} \frac{R_T}{r}\left[\frac{2\varepsilon_2 I_2'(2hr)\sin 2\phi}{B_0 - 2\varepsilon_2 I_2(2hr)\cos 2\phi}\right], & r > 0 \\ \frac{hR_T}{B_0}\varepsilon_2 \sin 2\phi\,, & r = 0 \end{cases}, \tag{29}$$

$$\hat{\iota} = \frac{R_T}{r}\frac{b_\theta}{b_z} = \begin{cases} \frac{2R_T}{hr^2}\left[\frac{\varepsilon_2 I_2(2hr)\cos 2\phi}{B_0 - 2\varepsilon_2 I_2(2hr)\cos 2\phi}\right], & r > 0 \\ \frac{hR_T}{B_0}\varepsilon_2 \cos 2\phi\,, & r = 0 \end{cases}, \tag{30}$$

where ε_2 depends on the radius of the helical coil [9]:

$$\varepsilon_2 = 2B_0 h a_c K_2'(\ell h a_c)\,. \tag{31}$$

Expanding $\psi(r,\phi)$ in Eq. (27) for small r, we find that the ratio of the axis of the elliptical, constant-ψ surfaces is given by

$$\varepsilon_\ell = \frac{a_1}{a_2} = \sqrt{\frac{1+\varepsilon_2/B_0}{1-\varepsilon_2/B_0}}\,.$$

In the limit $2hr \ll 1$, an expansion of I_2 gives $I_2(2hr) \sim [(2hr)^2/8]\,[1/(1+h^2r^2)]$ and $I_2'(2hr) \sim (2hr)/4$.

Figure 1 shows contours of constant $\psi(r,\phi)$ and $|B^0(r,\phi)|$ from Eqs. (27), (28), and (31). The parameters are those of the ATF stellarator:

$$\begin{aligned} \ell &= 2 \\ m &= 12 \\ L_p &= \frac{2\pi}{h} = 2.2 \text{ m helical field period length in } z \\ R_T &= 2.1 \text{ m} \\ B_0 &= 2\,T \\ a_c &= 0.46 \text{ m } (0.54 \text{ m used})\,. \end{aligned}$$

The coil radius a_c for ATF is 0.46 m, but to match the ATF ψ contours more accurately with the helically symmetric model, we take $a_c = 0.54$ m. Note that the positive value of L_p used here corresponds to a right-handed helix. The ATF device is actually a left-handed helix (negative L_p).

4 LOCAL ENERGY DEPOSITION AND ANTENNA IMPEDANCE

We rewrite the components of the electric field perpendicular to $\vec{B}$ in Eq. (12) as

$$\begin{aligned} E_\psi &= \frac{1}{|\nabla\hat{\psi}|}\left[E_r\left(\hat{\psi}_{,r} + hr\frac{b_r^2}{b_z}\right) + E_\theta\left(\hat{\chi}\frac{b_r}{b_\theta}\right)\right], \\ E_\chi &= \frac{1}{|\nabla\hat{\psi}|}\left(-E_r\frac{b_r}{b_z} + E_\theta\frac{\hat{\psi}_{,r}}{b_z}\right). \end{aligned} \tag{32}$$

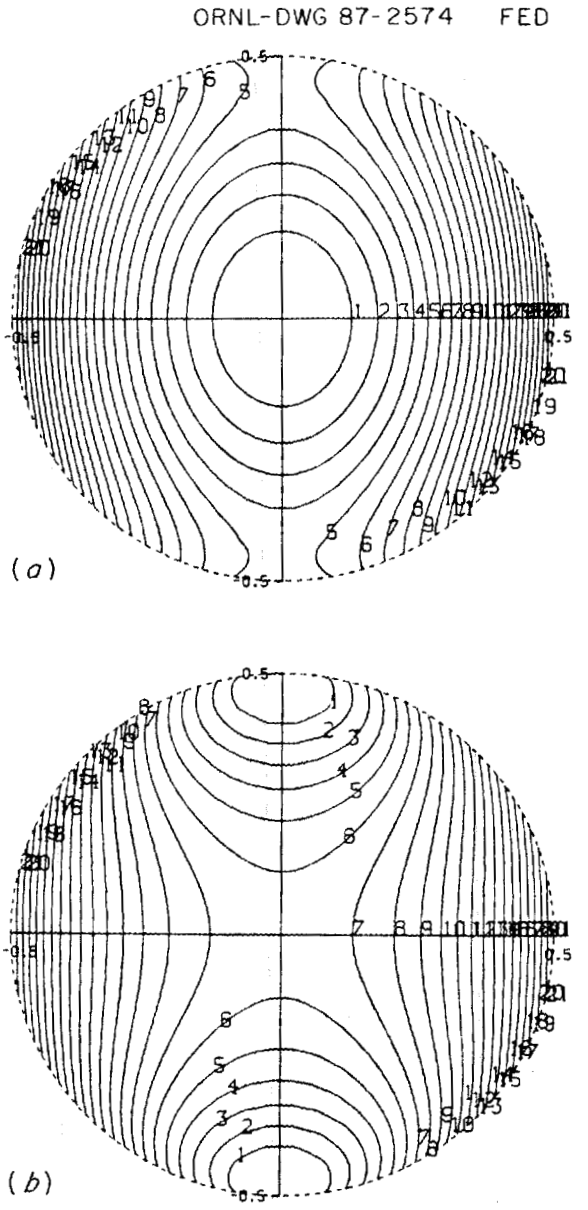

Figure 1: Helically symmetric magnetic field model for ATF: (a) contours of constant $\psi(r,\phi)$ and (b) contours of constant $|B(r,\phi)|$.

Now the plasma current can be written as

$$\vec{J}_{\text{plasma}} = \overleftrightarrow{\sigma} \cdot \vec{E} = -i\omega\varepsilon_0 \left(\overleftrightarrow{K} - \overleftrightarrow{I} \right) \cdot \vec{E} \,,$$

and we use Eq. (13) for $\overleftrightarrow{K} \cdot \vec{E}$ to get

$$\begin{aligned} \vec{J}_{\text{plasma}} = -i\omega\varepsilon \Big\{ & \hat{\delta}_1 \Big[(K_{xx} - 1) E_\psi + K_{xy} E_\chi \Big] \\ & + \hat{\delta}_2 \Big[K_{yx} E_y + (K_{yy} - 1) E_\chi \Big] + \hat{\delta}_3 \left(K_{zx} E_\psi + K_{zy} E_\chi \right) \Big\} \,. \end{aligned} \tag{33}$$

Now the local energy deposition rate is

$$\dot{W} = \frac{1}{2} \operatorname{Re} \left(\vec{E}^* \cdot \vec{J}_{\text{plasma}} \right) = \frac{1}{2} \operatorname{Re} \left(E_\psi^* J_{p,\psi} + E_\chi^* J_{p,\chi} + E_\parallel^* J_{p\parallel} \right) \,,$$

which with Eq. (33) and $E_\parallel = 0$ gives

$$\dot{W} = \frac{\omega\varepsilon_0}{2} \Big[\operatorname{Im}(K_{xx} - 1) |E_\psi|^2 + \operatorname{Im}(K_{yy} - 1) |E_\chi|^2 + 2 \operatorname{Re}(K_{xy}) \operatorname{Im}(E_\psi^* E_\chi) \Big] \,. \tag{34}$$

In the cold plasma case including collisions, $K_{xx} = K_{yy} = K_\perp$ and $K_{xy} = -iK_x$, so that

$$\dot{W} = \frac{\omega\varepsilon_0}{2} \Big[\operatorname{Im}(K_\perp - 1)(|E_\psi|^2 + |E_\chi|^2) + 2 \operatorname{Im} K_x \operatorname{Im}(E_\psi^* E_\chi) \Big] \,.$$

Now we define E^+ and E^- to be the left-hand and right-hand polarized waves respectively,

$$\begin{aligned} E_+ &= E_\psi + i E_\chi \, (\text{LHP}) \,, \\ E_- &= E_\psi - i E_\chi \, (\text{RHP}) \,. \end{aligned} \tag{35}$$

Then by defining

$$\begin{aligned} \sigma_{++} &= -i\omega\varepsilon_0 (L - 1) \,, \\ \sigma_{--} &= -i\omega\varepsilon_0 (R - 1) \,, \end{aligned} \tag{36}$$

where $L = \frac{1}{2}(K_{xx} + K_{yy}) + iK_{yx}$ and $R = \frac{1}{2}(K_{xx} + K_{yy}) - iK_{yx}$, we can write Eq. (34) equivalently as

$$\dot{W} = \frac{1}{4} \Big[\operatorname{Re}(\sigma_{++}) |E_+|^2 + \operatorname{Re}(\sigma_{--}) |E_-|^2 + \omega\varepsilon_0 \operatorname{Im}(K_{xx} - K_{yy}) \operatorname{Re} E_+^* E_- \Big] \,. \tag{37}$$

5 NUMERICAL RESULTS

In this section we present numerical solutions to the partial differential equations given in Eqs. (24) and (25). Figure 2 shows schematically the geometry treated. An elliptical plasma is contained within a perfectly conducting, straight, metal cylinder. There is low-density edge plasma between the wall and the main elliptical plasma. An external current with components $J_{\theta,\text{ext}}$ and $J_{z,\text{ext}}$ represents the antenna. The spatial distribution of this current is a delta function in r and a Gaussian of arbitrary width in $\phi = \theta - hz$. The

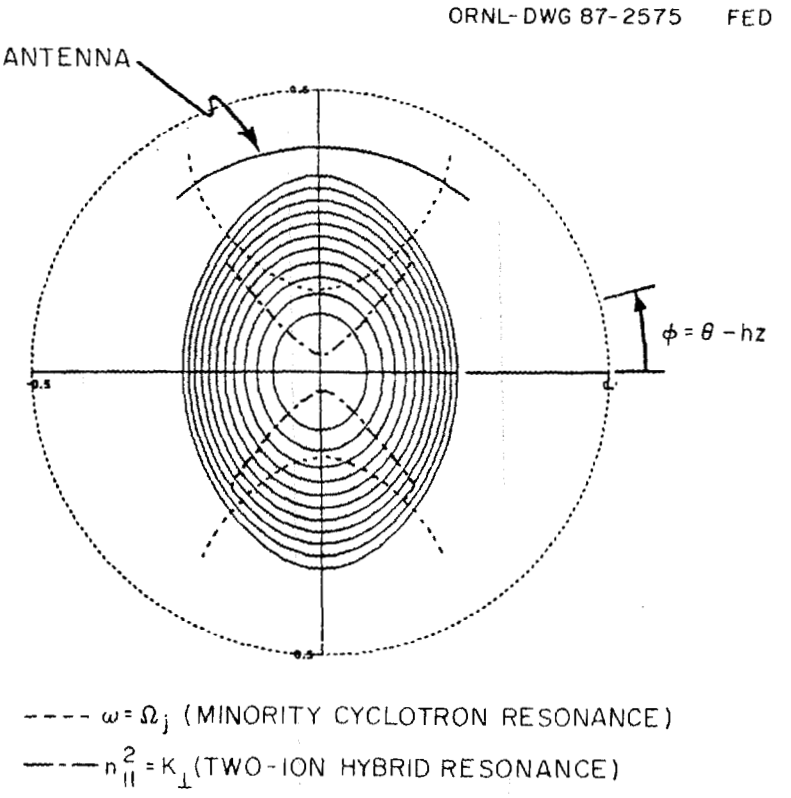

Figure 2: Straight helical geometry showing contours of constant density $n(r,\phi)$ (solid line),the two-ion hybrid resonance (chain-dashed line), and the minority cyclotron resonance (short-dashed line) for the ATF parameters of Table 1.

magnetic field is that shown in Fig. 1, and the density profile is taken constant on the flux surfaces of Fig. 1 with

$$n(\psi) = \begin{cases} (n_0 - n_s)(1 - \psi/\psi_b) + n_s\,, & \psi < \psi_b \\ n_s\,, & \psi > \psi_b \end{cases},$$

where ψ_b determines the plasma edge and n_s is the surface density. The dashed lines in Fig. 2 show the resonant surfaces for a minority hydrogen (5%), majority deuterium (95%) plasma. There are two minority hydrogen cyclotron resonance surfaces (short dash), which cross the vertical (y) axis above and below the horizontal plane. The applied frequency $f = 29.33$ MHz has been chosen so that the pair of two-ion hybrid resonances (chain-dash) cross the y-axis close to the origin at $r = 0$.

Figures 3–5 show results of solving Eqs. (24) and (25) for plasma parameters and antenna location typical of the ATF plasma in the minority hydrogen case (see Table 1). The finite difference mesh consists of 100 points in the radial direction ($0 < r < r_{\max}$) and 50 points poloidally ($0 < \phi < 2\pi$). Figure 3 shows contours of constant $|E_+(r,\phi)|$ and $|E_-(r,\phi)|$ for a case with $f = 28$ MHz. The outline of the elliptical plasma is clearly visible in Fig. 3(a) because E_+(LHP) tends to be shielded out of the plasma because of the ion cyclotron resonance; E_-, on the other hand, penetrates the plasma quite readily.

Figure 4 shows a sequence of power deposition contours $\dot{W}(r,\phi)$ and the flux surface average of the power absorbed $\langle \dot{W} \rangle_\psi$ as a function of y for three different applied frequencies $f = 28$, 30, and 31 MHz. At the lowest frequency, both pairs of resonant surfaces cross the vertical axis near the plasma edge, and the surface-averaged power deposition is peaked

ORNL-DWG 87-2576 FED

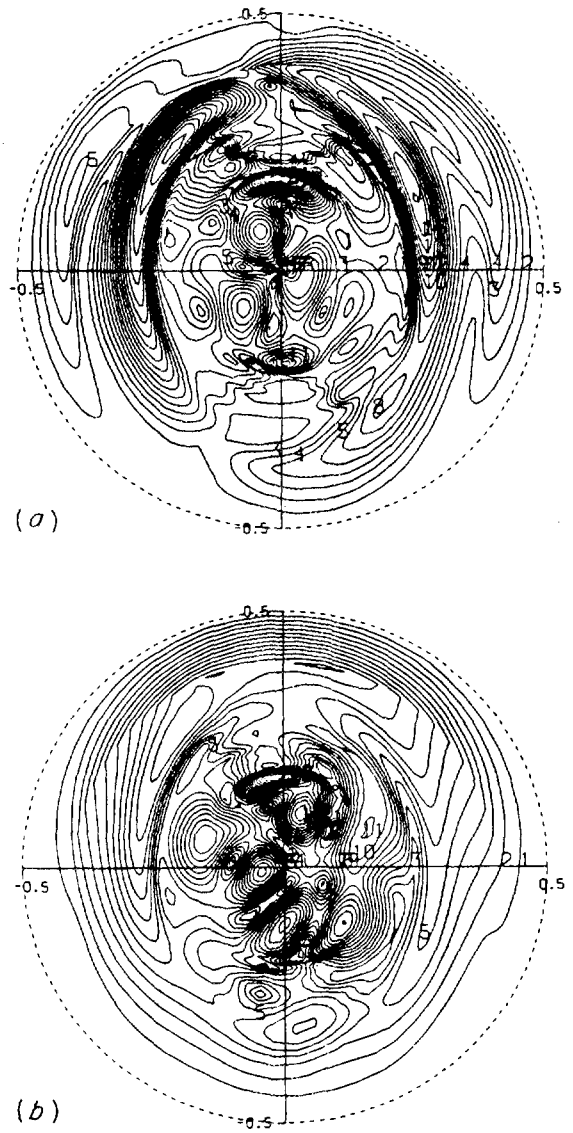

Figure 3: Contours of (a) constant $|E_+(r,\phi)|$ and (b) constant $|E_-(r,\phi)|$ for $f = 28$ MHz and parameters of Table 1.

fairly far off axis. Raising the frequency slightly causes the resonant surfaces to move closer to the axis, and power deposition becomes more nearly peaked near the plasma center. The best case, in fact, is 30 MHz, where because of the saddle point in $|B|$ the two-ion hybrid crosses the horizontal axis and the minority cyclotron resonance crosses the vertical axis. Finally, at 31 MHz both pairs of resonances cross the horizontal plane and power again is deposited only near the plasma periphery.

Another interesting result concerning the resonance structure shown by Fig. 4 is the tendency for power to be absorbed in thin layers along the flux surfaces rather than along the resonance contours themselves. This result was first noticed in tokamak geometry by

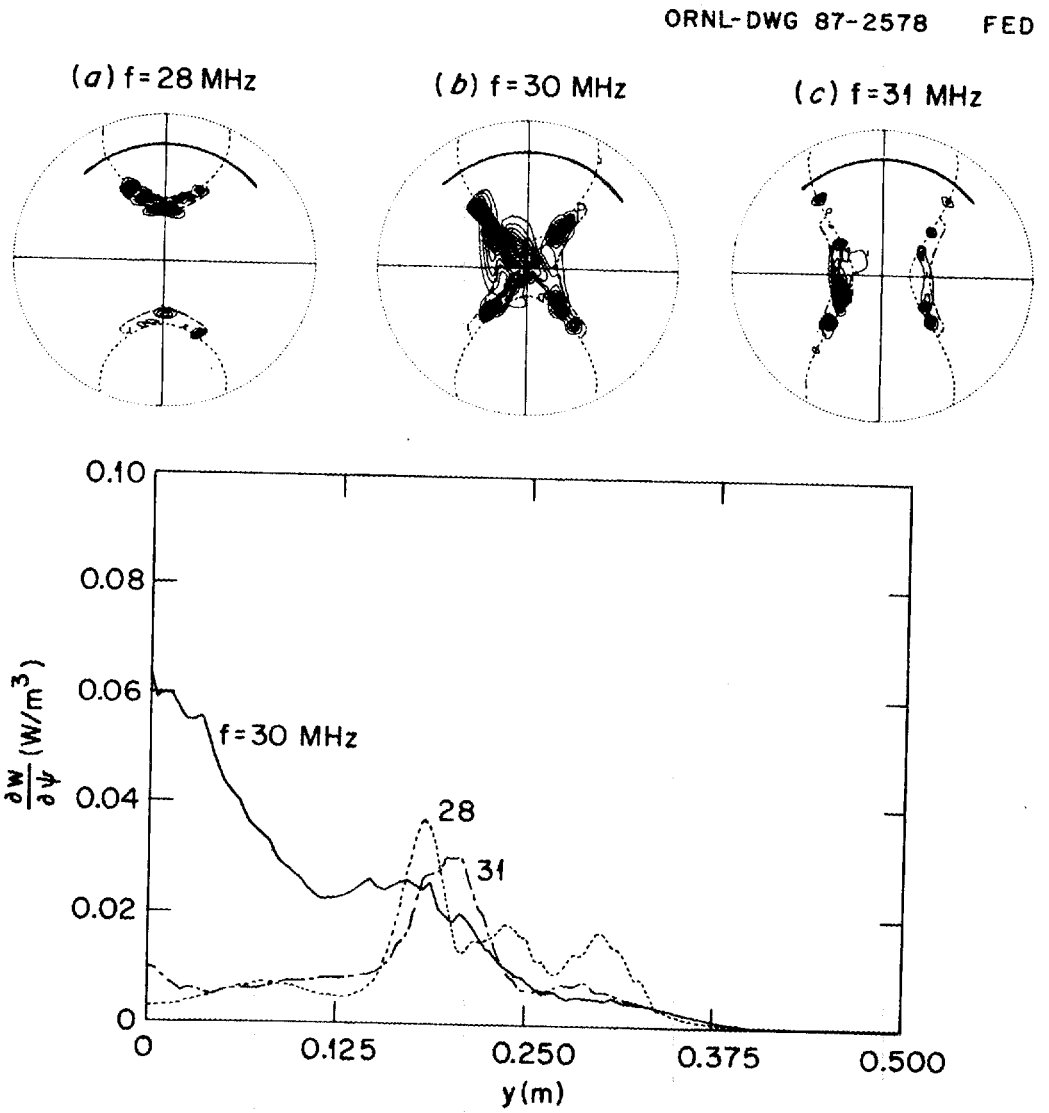

Figure 4: Contours of power deposition $\dot{W}(r,\phi)$ and flux surface average of power absorbed $\langle \dot{W} \rangle_\psi$ for $f = 28$, 30, and 31 MHz.

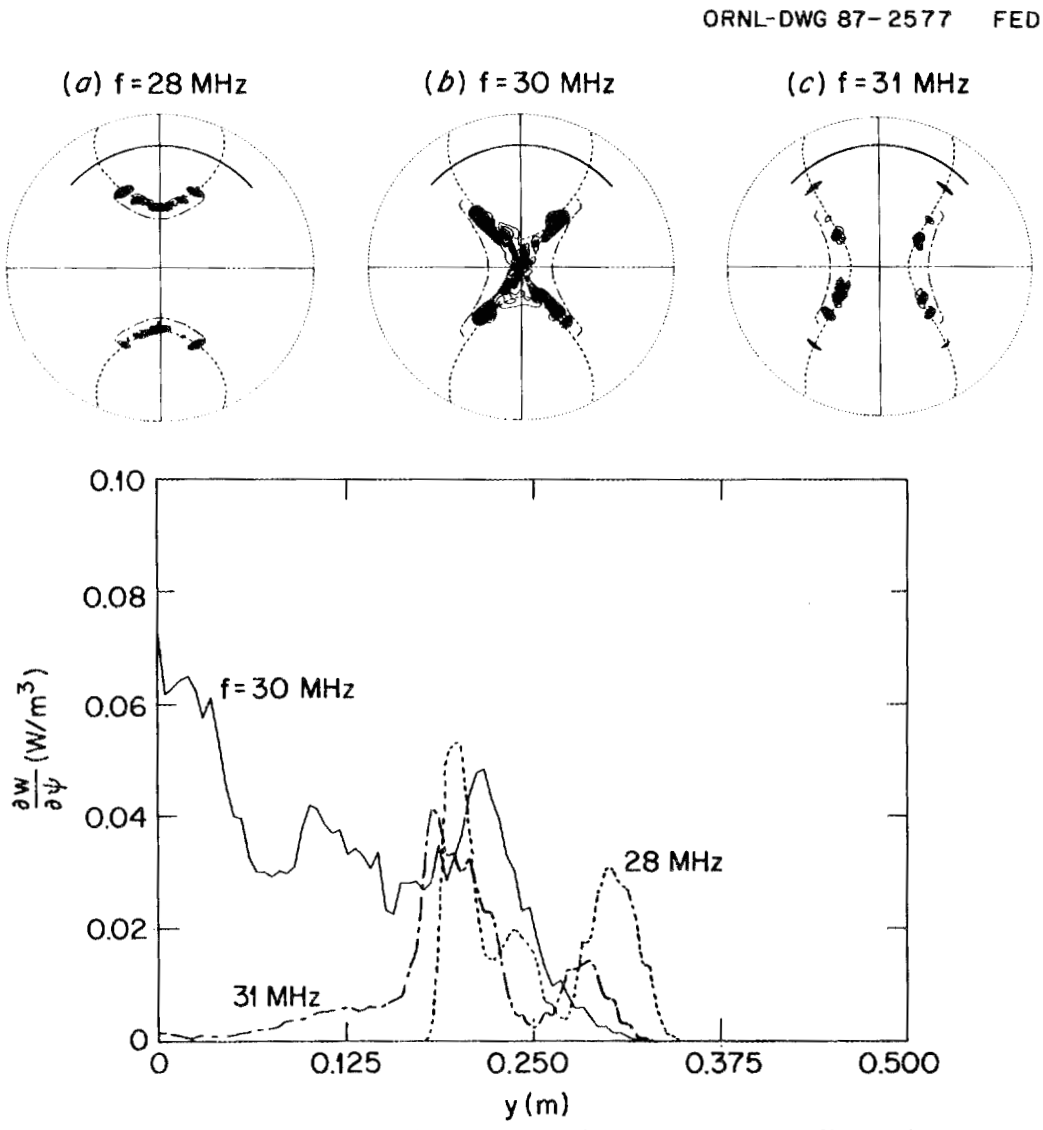

Figure 5: Same as Fig. 4, but for the lowest order warm plasma dielectric tensor, with $k_\perp \rho_i = 0$ and $k_\parallel = k_z$.

Hellsten and Tennfors [10], and we observe a similar effect in helical geometry. This effect is also evident in Fig. 5, where we replace the Lorentz collision model with the lowest order warm plasma dielectric tensor, assuming $k_\perp = 0$ and $k_\parallel = k_z$.

In Fig. 6 we consider parameters typical of the L-2 stellarator (see Table 2). Recent measurements on L-2 report efficient heating of a pure hydrogen plasma [11]. Thus, in Fig. 6 we compare (a) a pure hydrogen case to (b) a 5% minority hydrogen case for L-2. The total ion density in both cases is the same, $n = 10^{13}\,\mathrm{cm}^{-3}$. In Fig. 6(a), the total power absorbed, although comparable to that in the minority hydrogen case, is almost totally absorbed at the plasma edge. The electric field contours corresponding to this case show that E_+ is only a surface wave for the modes accessed by the plasma at this density, thus explaining the total lack of any central heating in Fig. 6(a). Whether or not it is possible to access other modes similar to $m = 1$ in mirrors remains to be seen.

ORNL-DWG 87-2579 FED

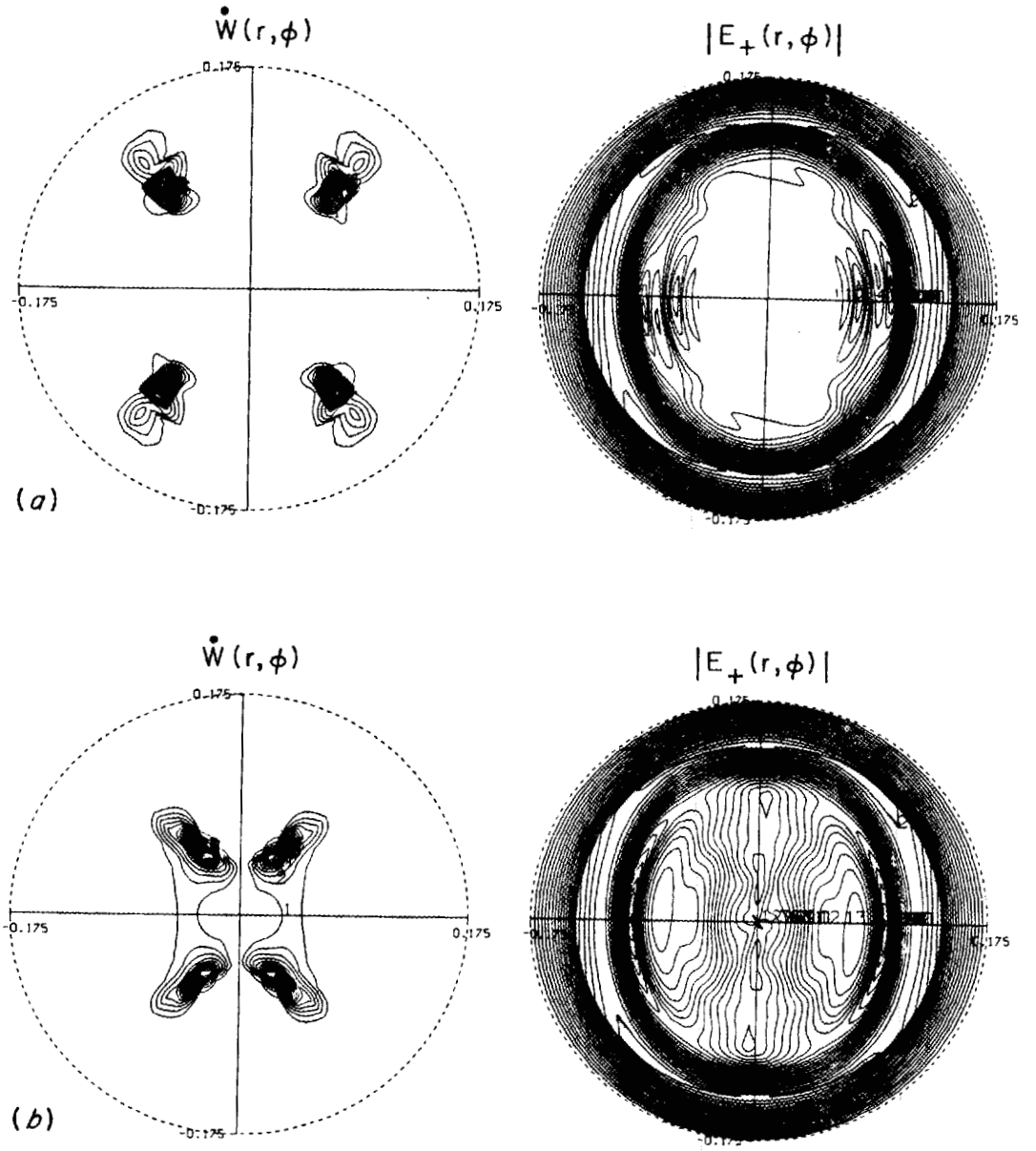

Figure 6: Power deposition and contours of constant $|E_+(r,\phi)|$ for the L-2 stellarator (Table 2) with (a) pure hydrogen and (b) 5% minority hydrogen in deuterium.

Table 1. Numerical Results for ATF Stellarator

$$\ell = 2, \quad m = 12$$

$$L_p = \frac{2\pi}{h} = 2.2\,\mathrm{m}$$

$$R_T = 2.1\,\mathrm{m}$$

$$B_0 = 2\,\mathrm{T}$$

$$a_{\mathrm{coil}} = 0.46\,\mathrm{m}\ (0.54\,\mathrm{m\,used})$$

$$\left.\begin{aligned} a_{1,\mathrm{plasma}} &= 0.27\,\mathrm{m} \\ a_{2,\mathrm{plasma}} &= 0.38\,\mathrm{m} \end{aligned}\right\} \varepsilon = \frac{a_{1,\mathrm{plasma}}}{a_{2,\mathrm{plasma}}} \sim 0.84$$

$$a_{\mathrm{antenna}} = 0.40\,\mathrm{m}$$

$$\left.\begin{aligned} n(\mathrm{H}) &= 2 \times 10^{12}\,\mathrm{cm}^{-3} \\ n(\mathrm{D_2}) &= 4 \times 10^{13}\,\mathrm{cm}^{-3} \end{aligned}\right\} \eta = \frac{n(\mathrm{H})}{n(\mathrm{D_2})} = 0.05$$

$$n_s = 4 \times 10^{11}\,\mathrm{cm}^{-3}$$

$$f = \frac{\omega}{2\pi} \sim 30\ \mathrm{MHz}$$

$$k_z R_T = n_{\mathrm{toroidal}} = 8$$

$$\frac{\nu}{\omega} \sim 5 \times 10^{-3}$$

Table 2. Parameters for L-2 Calculations

$$\ell = 2, \quad m = 14$$

$$L_p = \frac{2\pi}{h} = 0.8976\,\mathrm{m}$$

$$R_T = 1.0\,\mathrm{m}$$

$$B_0 = 1.2\,\mathrm{T}$$

$$a_{\mathrm{coil}} = 0.175\,\mathrm{m}\ (0.225\ \mathrm{used})$$

$$\left.\begin{aligned} a_{1,\mathrm{plasma}} &= 0.105 \\ a_{2,\mathrm{plasma}} &= 0.125 \end{aligned}\right\} \varepsilon = \frac{a_{1,\mathrm{plasma}}}{a_{2,\mathrm{plasma}}} \sim 0.84$$

$$a_{\mathrm{antenna}} = 0.1396\,\mathrm{m} \quad (m = 0, \text{symmetric in } \phi)$$

$$\left.\begin{aligned} n(\mathrm{H}) &= 0.05 \times 10^{13}\,\mathrm{cm}^{-3} \\ n(\mathrm{D_2}) &= 0.95 \times 10^{13}\,\mathrm{cm}^{-3} \end{aligned}\right\} \eta = \frac{n(\mathrm{H})}{n(\mathrm{D_2})}$$

$$n_s = 1 \times 10^{11}\,\mathrm{cm}^{-3}$$

$$f = \frac{\omega}{2\pi} = 18\ \mathrm{MHz}$$

$$k_z R_T = -5$$

$$\frac{\nu}{\omega} = 5 \times 10^{-3}$$

REFERENCES

[1] V. A. Batyuk et al., *Proceedings of the 11th European Conferences on Controlled Fusion and Plasma Physics, Aachen, 1983*, p. 373, European Physical Society, 1983.

[2] F. W. Perkins, *IEEE Trans. Plasma Sci.* **PS-12**, 53 (1984).

[3] L. M. Kovrizhnykh and P. E. Moroz, *Sov. Phys.–Tech. Phys.* **29**, 384 (1984).

[4] L. M. Kovrizhnykh and P. E. Moroz, *Sov. Phys. JETP* **60**, 946 (1984).

[5] A. Fukayama, N. Okazaki, A. Goto, S. I. Itoh, and K. Itoh, *Nucl. Fusion* **26**, 151 (1986).

[6] E. F. Jaeger, D. B. Batchelor, H. Weitzner, and J. H. Whealton, *Comput. Phys. Commun.* **40**, 33 (1986).

[7] J. L. Johnson, C. R. Oberman, R. M. Kulsrud, and E. A. Frieman, *Phys. Fluids* **1**, 281 (1958).

[8] K. Miyamoto, *Nucl. Fusion* **18**, 243 (1978).

[9] C. Chu, M. J. Schaffer, R. J. La Haye, and T. Ohkawa, *IEEE Trans. Plasma Sci.* **PS-9**, 187 (1981).

[10] T. Hellsten and E. Tennfors, *Phys. Scr.* **30**, 341 (1984).

[11] L. Villard, K. Appert, R. Gruber, and J. Vaclavik, *Comput. Phys. Rep.* **4**, 95 (1986).

ORNL/TM-10223
Dist. Category UC-20 g

INTERNAL DISTRIBUTION

1. D. B. Batchelor
2. C. O. Beasley
3. B. A. Carreras
4. M. D. Carter
5. E. C. Crume
6. N. O. Dominguez
7. R. A. Dory
8. C. L. Hedrick
9. S. P. Hirshman
10. J. T. Hogan
11. W. A. Houlberg
12. H. C. Howe
13. E. F. Jaeger
14. J-N. Leboeuf
15. G. S. Lee
16. J. F. Lyon
17. J. A. Rome
18. K. C. Shaing
19. J. Sheffield
20. D. A. Spong

21-22. Laboratory Records Department
23. Laboratory Records, ORNL-RC
24. Document Reference Section
25. Central Research Library
26. Fusion Energy Division Library
27–28. Fusion Energy Division Publications Office
29. ORNL Patent Office

EXTERNAL DISTRIBUTION

30. Office of the Assistant Manager for Energy Research and Development, U.S. Department of Energy, Oak Ridge Operations Office, P. O. Box E, Oak Ridge, TN 37831
31. J. D. Callen, Department of Nuclear Engineering, University of Wisconsin, Madison, WI 53706-1687
32. J. F. Clarke, Director Office of Fusion Energy, Office of Energy Research, ER-50 Germantown, U.S. Department of Energy, Washington, DC 20545
33. R. W. Conn, Department of Chemical, Nuclear, and Thermal Engineering, University of California, Los Angeles, CA 90024
34. S. O. Dean, Fusion Power Associates, 2 Professional Drive, Suite 248, Gaithersburg, MD 20879
35. H. K. Forsen, Bechtel Group, Inc., Research Engineering, P. O. Box 3965, San Francisco, CA 94105
36. J. R. Gilleland, GA Technologies, Inc., Fusion and Advanced Technology, P.O. Box 81608, San Diego, CA 92138
37. R. W. Gould, Department of Applied Physics, California Institute of Technology, Pasadena, CA 91125
38. R. A. Gross, Plasma Research Laboratory, Columbia University, New York, NY 10027
39. D. M. Meade, Princeton Plasma Physics Laboratory, P.O. Box 451, Princeton, NJ 08544
40. M. Roberts, International Programs, Office of Fusion Energy, Office of Energy Research, ER-52 Germantown, U.S. Department of Energy, Washington, DC 20545
41. W. M. Stacey, School of Nuclear Engineering and Health Physics, Georgia Institute of Technology, Atlanta, GA 30332

42. D. Steiner, Nuclear Engineering Department, NES Building, Tibbetts Avenue, Rensselaer Polytechnic Institute, Troy, NY 12181
43. R. Varma, Physical Research Laboratory, Navrangpura, Ahmedabad 380009, India
44. Bibliothek, Max-Planck Institut fur Plasmaphysik, D-8046 Garching, Federal Republic of Germany,
45. Bibliothek, Institut fur Plasmaphysik, KFA, Postfach 1913, D-5170 Julich, Federal Republic of Germany,
46. Bibliotheque, Centre de Recherches en Physique des Plasmas, 21 Avenue des Bains, 1007 Lausanne, Switzerland
47. F. Prevot, CEN/Cadarache, Departement de Recherches sur la Fusion Controlee, F-13108 Saint-Paul-lez-Durance Cedex, France
48. Documentation S.I.G.N., Departement de la Physique du Plasma et de la Fusion Controlee, Centre d'Etudes Nucleaires, B.P. 85, Centre du Tri, F-38041 Grenoble, France
49. Library, Culham Laboratory, UKAEA, Abingdon, Oxfordshire, OX14 3DB, England
50. Library, FOM-Instituut voor Plasma-Fysica, Rijnhuizen, Edisonbaan 14, 3439 MN Nieuwegein, The Netherlands
51. Library, Institute of Plasma Physics, Nagoya University, Nagoya 464, Japan
52. Library, International Centre for Theoretical Physics, P.O. Box 586, I-34100 Trieste, Italy
53. Library, Laboratorio Gas Ionizatti, CP 56, I-00044 Frascati, Rome, Italy
54. Library, Plasma Physics Laboratory, Kyoto University, Gokasho, Uji, Kyoto, Japan
55. Plasma Research Laboratory, Australian National University, P.O. Box 4, Canberra, A.C.T. 2000, Australia
56. Thermonuclear Library, Japan Atomic Energy Research Institute, Tokai Establishment, Tokai-mura, Naka-gun, Ibaraki-ken, Japan
57. G. A. Eliseev, I. V. Kurchatov Institute of Atomic Energy, P.O. Box 3402, 123182 Moscow, U.S.S.R.
58. V. A. Glukhikh, Scientific-Research Institute of Electro-Physical Apparatus, 188631 Leningrad, U.S.S.R.
59. I. Shpigel, Institute of General Physics, U.S.S.R. Academy of Sciences, Ulitsa Ulitsa Vavilova 38, Moscow, U.S.S.R.
60. D. D. Ryutov, Institute of Nuclear Physics, Siberian Branch of the Academy of Sciences of the U.S.S.R., Sovetskaya St. 5, 630090 Novosibirsk, U.S.S.R.
61. V. T. Tolok, Kharkov Physical-Technical Institute, Academical St. 1, 310108 Kharkov, U.S.S.R.
62. Library, Academia Sinica, P.O. Box 3908, Beijing, China (PRC)
63. D. Crandall, Experimental Plasma Research Branch, Division of Development and Technology, Office of Fusion Energy, Office of Energy Research, ER-542 Germantown, U.S. Department of Energy, Washington, DC 20545
64. N. A. Davies, Office of the Associate Director, Office of Fusion Energy, Office of Energy Research, ER-51 Germantown, U.S. Department of Energy, Washington, DC 20545

65. D. B. Nelson, Director, Division of Applied Plasma Physics, Office of Fusion Energy, Office of Energy Research, ER-54 Germantown, U.S. Depart ment of Energy, Washington, DC 20545

66. E. Oktay, Division of Confinement Systems, Office of Fusion Energy, Office of Energy Research, ER-55 Germantown, U.S. Department of Energy, Washington, DC 20545

67. W. Sadowski, Fusion Theory and Computer Services Branch, Division of Applied Plasma Physics, Office of Fusion Energy, Office of Energy Research, ER-541 Germantown, U.S. Department of Energy, Washington, DC 20545

68. P. M. Stone, Fusion Systems Design Branch, Division of Development and Technology, Office of Fusion Energy, Office of Energy Research, ER-532 Germantown, U.S. Depart ment of Energy, Washington, DC 20545

69. J. M. Turner, International Programs, Office of Fusion Energy, Office of Energy Research, ER-52 Germantown, U.S. Depart ment of Energy, Washington, DC 20545

70. R. E. Mickens, Atlanta University, Department of Physics, Atlanta, GA 30314

71. M. N. Rosenbluth, RLM 11.218, Institute for Fusion Studies, University of Texas, Austin, TX 78712

72. Duk-In Choi, Department of Physics, Korea Advanced Institute of Science and Technology, P.O. Box 150, Chong Ryang-Ri, Seoul, Korea

73. Theory Department Read File, c/o D. W. Ross, University of Texas, Institute for Fusion Studies, Austin, TX 78712

74. Theory Department Read File, c/o R. C. Davidson, Director, Plasma Fusion Center, NW 16-202, Massachusetts Institute of Technology, Cambridge, MA 02139

75. Theory Department Read File, c/o R. White, Princeton Plasma Physics Laboratory, P.O. Box 451, Princeton, NJ 08544

76. Theory Department Read File, c/o L. Kovrizhnykh, Lebedev Institute of Physics, Academy of Sciences, 53 Leninsky Prospect, 117924 Moscow, U.S.S.R.

77. Theory Department Read File, c/o B. B. Kadomtsev, I. V. Kurchatov Institute of Atomic Energy, P.O. Box 3402, 123182 Moscow, U.S.S.R.

78. Theory Department Read File, c/o T. Kamimura, Institute of Plasma Physics, Nagoya University, Nagoya 464, Japan

79. Theory Department Read File, c/o C. Mercier, Departemente de Recherches sur la Fusion Controlee, B.P. No. 6, F-92260 Fontenay-aux-Roses (Seine), France

80. Theory Department Read File, c/o T. E. Stringer, JET Joint Undertaking, Culham Laboratory, Abingdon Oxfordshire, OX14 3DB, England

81. Theory Department Read File, c/o R. Briscoe, Culham Laboratory, Abingdon, Oxfordshire OX14 3DB, England

82. Theory Department Read File, c/o D. Biskamp, Max-Planck-Institut fur Plasmaphysik, D-8046 Garching, Federal Republic of Germany

83. Theory Department Read File, c/o T. Takeda, Japan Atomic Energy Research Institute, Tokai Establishment, Tokai-mura, Naka-gun, Ibaraki-ken, Japan

84. Theory Department Read File, c/o J. Greene, GA Technologies, Inc., P.O. Box 81608, San Diego, CA 92138

85. Theory Department Read File, c/o L. D. Pearlstein, L-630, Lawrence Livermore National Laboratory, P.O. Box 5511, Livermore, CA 94550

86. Theory Department Read File, c/o R. Gerwin, CTR Division, Los Alamos National Laboratory, P.O. Box 1663, Los Alamos, NM 87545

87. C. D. Boley, Fusion Power Program, Bldg. 207C, Argonne National Laboratory, Argonne, IL 60439,

88. C. De Palo, Library, Associazione EURATOM-ENEA sulla Fusione, CP 65, I-00044 Frascati (Roma), Italy

89. P. H. Diamond, Institute for Fusion Studies, University of Texas, Austin, TX 78712

90. Yu. N. Dnestrovskij, I. V. Kurchatov Institute of Atomic Energy, P.O. Box 3402, 123182 Moscow, U.S.S.R.

91. A. Fruchtman, Courant Institute of Mathematical Physics, New York University, 251 Mercer Street, New York, NY 10012

92. J. Gaffey, IPST, University of Maryland, College Park, MD 20742

93. R. J. Hawryluk, Princeton Plasma Physics Laboratory, P.O. Box 451, Princeton, NJ 08544

94. D. G. McAlees, Advanced Nuclear Fuels Corporation, 600 108th Avenue N.E., Bellevue, WA 98009

95. W. W. Pfeiffer, GA Technologies, Inc., P.O. Box 85608, San Diego, CA 92138

96. D. E. Post, Princeton Plasma Physics Laboratory, P.O. Box 451, Princeton, NJ 08544

97. P. J. Reardon, Princeton Plasma Physics Laboratory, P.O. Box 451, Princeton, NJ 08544

98. K. Riedel, Courant Institute of Mathematical Physics, New York University, 251 Mercer Street, New York, NY 10012

99. A. Ware, Department of Physics, University of Texas, Austin, TX 78712

100. H. Weitzner, Courant Institute of Mathematical Physics, New York University, 251 Mercer Street, New York, NY 10012

101. J. Wiley, Institute for Fusion Studies, University of Texas, Austin, TX 78712

102. S. K. Wong, GA Technologies, Inc., P.O. Box 85608, San Diego, CA 92138

103. S. Yoshikawa, Princeton Plasma Physics Laboratory, P.O. Box 451, Princeton, NJ 08544

104–224. Given distribution according to TIC-4500 Magnetic Fusion Energy (Category Distribution UC-20g Theoretical Plasma Physics)